Journal of Thermal Analysis and Calorimetry, Vol. 83 (2006) 2, 457–462

TG/DTA/MS STUDY OF THE THERMAL DECOMPOSITION OF $FeSO_4 \cdot 6H_2O$

P. Masset[1,2,3]*, *J.-Y. Poinso*[1] *and J.-C. Poignet*[3]

[1]Commissariat à l'Energie Atomique, Centre d'Etude du Ripault, BP 16, 37260 Monts, France
[2]ASB – Aerospatiale Batteries, Allée Sainte Hélčne, 18021 Bourges, France
[3]Laboratoire d'Electrochimie et de Physicochimie des Matériaux et Interfaces (LEPMI), 1130 rue de la Piscine, BP 75 38402 Saint Martin d'Hčres, France

The thermal decomposition of $FeSO_4 \cdot 6H_2O$ was studied by mass spectroscopy coupled with DTA/TG thermal analysis under inert atmosphere. On the ground of TG measurements, the mechanism of decomposition of $FeSO_4 \cdot 6H_2O$ is:
i) three dehydration steps

$$FeSO_4 \cdot 6H_2O \xrightarrow{70-100°C} FeSO_4 \cdot 4H_2O + 2H_2O$$

$$FeSO_4 \cdot 4H_2O \xrightarrow{95-190°C} FeSO_4 \cdot H_2O + 3H_2O$$

$$FeSO_4 \cdot H_2O \xrightarrow{245-310°C} FeSO_4 + H_2O$$

ii) two decomposition steps

$$6FeSO_4 \xrightarrow{525-650°C} Fe_2(SO_4)_3 + 2Fe_2O_3 + 2SO_2$$

$$Fe_2(SO_4)_3 \xrightarrow{625-710°C} Fe_2O_3 + 3SO_2 + 3/2O_2$$

The intermediate compound was identified as $Fe_2(SO_4)_3$ and the final product as the hematite Fe_2O_3.

Keywords: *DTA/TG, dehydration, $FeSO_4 \cdot 6H_2O$, mass spectrometry*

Introduction

Pyrite FeS_2 is commonly used as cathode material [1] in Li–Al//FeS_2 thermally activated batteries (thermal batteries) due to *i*) its redox properties: discharge potential around 1.8 V *vs.* Li–Al reference electrode at 450°C [2] , *ii*) its thermal stability up to 600°C [3–5], *iii*) and its low cost: 0.5$/kg of FeS_2 [6]. The natural iron disulfide FeS_2 is obtained by ore treatment. Usually, chemical and thermal treatments are carried out to reduce natural impurities. Nevertheless, sulphate impurities may still be present on pyrite surface. Natural oxidation of transition metal sulphides is known to lead to sulphates species. Sulphate crystal growth has been revealed by XPS analysis on fresh surface of synthetic pyrite [4]. For the thermal battery application, a 'voltage spike' is generally observed at the beginning of the discharge. It is due to the presence of some oxidised species on the pyrite surface. Iron sulfate may be involved in this process. To cut-off the 'voltage spike', oxides (Li_2O), sulphides (Li_2S) [7, 8] are added to the cathode mixture (molten salt+FeS_2). Sulphur could be used too [9]. Thermal stability studies of FeS_2 samples revealed mass losses in the 500–550°C temperature range. They were ascribed to the thermal decomposition of hydrated iron sulphates. Wheeler *et al.* [10] studied the dehydration process of ferrous sulphate heptahydrate. Under vacuum at 40°C, the dehydration results in a smooth continuous mass loss, the end product having the composition of the monohydrate. Gallagher *et al.* [11] showed that dehydration of $FeSO_4 \cdot 7H_2O$ occurred at about 250°C. The $FeSO_4 \cdot H_2O$ decomposition temperature of 285 and 288°C was determined by Pannetier *et al.* [12] and Safiullin *et al.* [13], respectively. Dehydration of $FeSO_4 \cdot H_2O$ takes place at 220°C under inert atmosphere [14] as well as under CO atmosphere.

Recently, dehydration kinetic of $FeSO_4 \cdot 7H_2O$ was carefully studied by Kanari *et al.* [15] by isothermal and non isothermal DTA/TG experiments under neutral, oxidizing and chlorinating atmospheres. Under vacuum, they proposed the sequence of dehydration for $FeSO_4 \cdot 7H_2O$ crystals as 2, 3 and 1 moles of water removed at temperatures of 70, 95 and 245°C. For the first two steps, the apparent activation energies were equal to 72 and 83 kJ mol^{-1}, respectively. The apparent activation energy was not calculated for the third step. The reaction pathway for the decomposition of $FeSO_4$ was subjected to some controversy. The final product of the thermal decomposition of iron sulphate was well identi-

* Author for correspondence: masset@dechema.de

1388–6150/$20.00

Akadémiai Kiadó, Budapest, Hungary
Springer, Dordrecht, The Netherlands

fied as magnetite Fe_2O_3 with its typical reddish colour. Other important features of the $FeSO_4$ decomposition reaction include reaction temperature range and intermediate products. Because, sulphurs can react with the molten salt phase, they should be integrated in the thermodynamic calculations [16] to predict accurately the battery behaviour during the thermal activation step. Earlier, the $FeSO_4$ thermal decomposition was studied by several authors [11–13]. Gallagher [11] showed that, under nitrogen atmosphere, $Fe_2O_2SO_4$ was formed in the 475–575°C temperature range. Pannetier *et al.* [12], and Safiullin *et al.* [13] showed that $Fe_2(SO_4)_3$ was formed at 618 and 687°C, respectively. The same authors determined that $Fe_2(SO_4)_3$ decomposes to Fe_2O_3 at 768 and 755°C, respectively. These temperatures are 100°C higher than those measured by Gallagher *et al*. [11]. Recently, Siriwardane *et al.* [17] detected only $Fe_2(SO_4)_3$ as intermediate product during the decomposition of $FeSO_4$. In the course of this work but published earlier, the decomposition pyrite FeS_2, iron(II) sulphate heptahydrate and iron(III) hydrate was investigated by Thomas *et al.* [18] using a mass spectrometer coupled to a thermal analyser. By mass spectrometry, they confirmed the two-step decomposition mechanism of $FeSO_4$ with the formation of $Fe_2(SO_4)_3$ as intermediate product.

In the frame of internal project, the study of the thermal decomposition of $FeSO_4 \cdot xH_2O$ was undertaken under inert atmosphere in order to determine the reaction temperature range, and the nature of the resulting intermediate and the final product.

Experimental

Materials

The iron sulphate hydrate $FeSO_4 \cdot 6H_2O$ (purity+98%), taken from the available LEPMI's chemicals inventory, was purchased from Sigma-Aldrich. Samples were prepared in a glove box under high purity argon (moisture and oxygen contents were typically less than 1 ppm). They were used without further treatment. Pyrite FeS_2 was provided by ASB-Aerospatiale Batteries. It was used without any further chemical or thermal treatments. It was stored under high purity argon atmosphere (<1 ppm of O_2 and H_2O) in glove box. It was sieved and only the particles in the 40–200 μm size range were kept.

Methods

Elemental analysis

The elemental analysis of $FeSO_4 \cdot 6H_2O$ and FeS_2 was carried out. Iron content was determined by standard atomic absorption spectroscopy technique ICP-EAS. Sulphur, hydrogen and oxygen contents were determined using the carbothermal oxidation. The $FeSO_4/H_2O$ ratio (e.g. crystallization water molecules) in the $FeSO_4 \cdot 6H_2O$ crystals was checked.

Oxygen content was measured by means oxide analysis. Experiments were carried out with a LECO TC-436. Oxygen of the sample reacts with the carbon crucible to produce carbon monoxide, at high temperature and during a short time. Then, CO is transformed into CO_2 by oxidation in a CuO tower. And finally, the CO_2 level is measured by an infrared cell. Sample mass was close to 1 mg.

X-ray diffraction

X-ray powder diffraction analysis of the parent reactants together with their decomposition solid products was carried out using a Siemens D500 diffractometer, using CoKα radiation (λ=1.789 Å) equipped with a linear detector. X-ray diffraction was performed on samples protected by a polyethylene film to prevent reaction with water and/or oxygen during the analysis. Phase identification was done using the JCPDS sheet library available on the data acquisition system.

Thermal analysis

Thermal analyses consisted in TG-DTG-DTA measurements. They were performed using a Setaram 24 thermal analyser equipped with a double oven in order to optimise the TG measurements. Experiments were carried out in dynamic atmosphere (flow rate of 50 cm^3 min^{-1}) of dry helium (less than 1 ppm H_2O). Constant sample mass (85±1 mg) was used to reduce the influence of the mass on the measurements (DTA or DTG peak shapes and temperatures of maxima used in calculations). Samples were crushed in agate mortar and then stored under inert atmosphere. During the experiments, samples were contained in 100 μL Al_2O_3 alumina crucibles. Prior to use, the crucibles were washed with water in an ultrasonic bath during 30 min, rinsed with acetone, then dried at 120°C overnight in an oven, and finally transferred in a glove-box.

Mass spectrometry analysis

A quadripole Balzers mass spectrometer was connected directly to the gas exhaust pipe of the thermal analyser. The ratio m/q (ionic species mass on charge) available ranged between 0 and 200. The volatile reaction products were continuously sampled by means of a gas-sampling apparatus situated in the thermal analyser. A thin capillary (heated at 120°C) ensured the connection between the analysis chamber of the mass spectrometer and the thermal analyser. For each species, intensity ratio of the peak were checked and

compared to the reference data sheets contained in the database of the software.

A first batch of experiments was realised by recording the 200 *m*/*q* ratio available. After, only the sensitive *m*/*q* ratio were recorded during a second set of experiments.

Results and discussion

FeS_2 and $FeSO_4 \cdot 6H_2O$ characterisation

Elemental analysis was carried out to evaluate the elemental composition of the $FeSO_4 \cdot 6H_2O$ sample and the $FeSO_4/H_2O$ molar ratio. Coupling the ICP-AES and the carbothermal oxidation techniques, it allows the determination of the $FeSO_4/H_2O$ molar ratio of the original compound. The composition of the original sample is $FeSO_4 \cdot 6H_2O$. The mass composition of each element is reported in Table 1. For the hydrogen content, discrepancy close to 10% was noticed between our experimental value and the expected theoretical one. On the overall, our results agree with the proposed composition with an accuracy better than 2%.

Iron, sulphur, oxygen and hydrogen contents were determined to evaluate the FeS_2 sample impurity level. The values and techniques used are summarised in Table 1. The Fe/S molar ratio was found to be 1.136. It means our pyrite, with the $FeS_{1.98}$ composition, is slightly deficient in sulphur. Usually, this composition is linked to the origin of the natural mineral of pyrite. In addition to the pyrite phase, hydrated sulfate $FeSO_4 \cdot xH_2O$ was detected by means of X-ray diffraction. In addition, sulfate species were also detected by mass spectrometry coupled with DTA/TG thermal analysis. At temperatures close to 125, 230 and 525°C, mass losses were observed but they could not be ascribed to the FeS_2 thermal decomposition reaction (Fig. 1). The mass losses were attributed to sulfate decomposition on the pyrite surface. These observations agree with previous studies [19].

Thermal decomposition reaction mechanism

As shown in Fig. 2, the thermal decomposition of $FeSO_4 \cdot 6H_2O$ proceeds via five steps ranging from 70 and up to 650°C with clearly defined thermal events.

Table 1 Iron, sulphur, oxygen and hydrogen elemental analysis of the $FeSO_4 \cdot 6H_2O$ sample

Elements/%	$FeSO_4 \cdot 6H_2O$	FeS_2	Techniques
Fe	21.7 (21.54)	45.3±1.8	ICP-AES
S	12.5 (12.31)	56.8±5.7	Carb. ox
O	61.6 (61.53)	1.5±0.4	Carb. ox
H	4.2 (4.61)	15 (ppm)	Carb. ox

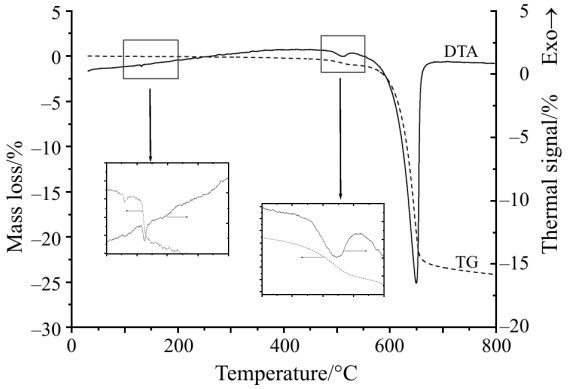

Fig. 1 TG and DTA curve recorded at 5°C min^{-1} of FeS_2

The five decomposition steps were identified as three dehydration reactions followed by the two-step thermal decomposition of the $FeSO_4$ compound. The dehydration processes occurred between 70 and 250°C. They will respectively be referenced as dehyd 1 (low temperature), dehyd 2 (medium temperature) and dehyd 3 (high temperature). They were followed by the two decomposition steps of the dehydrated iron sulphate, which will be called decomp 1 and decomp 2 (low and high temperature, respectively).

A set of TG curves were recorded for different heating rates ranging between 1 and 20°C min^{-1} (Fig. 3). All the mass variations cited in the text are given with respect to the mass of the initial $FeSO_4 \cdot 6H_2O$ compound (Table 2). For each step, five values of mass variations were recorded by TG at different heating rates.

The proposed mechanism of $FeSO_4 \cdot 6H_2O$ thermal decomposition detailed hereafter is based on the mass variations. In addition, XRD experiments were carried out to check the phase formed. Mass spectrometry coupled to the DTA/TG analyser was used to identify the species issued from the thermal decomposition of the $FeSO_4 \cdot 6H_2O$ compound. It should be mentioned that the mass variation measurements become less sensitive

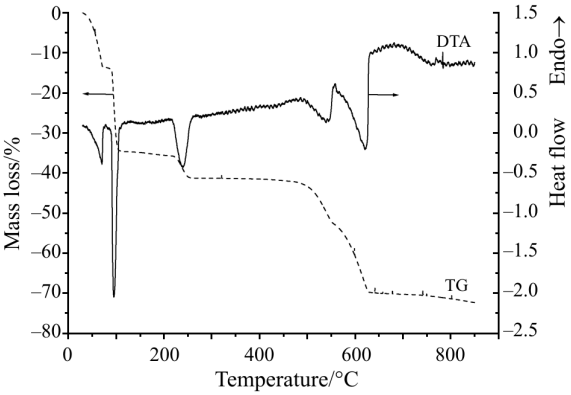

Fig. 2 TG and DTA curves recorded at 1°C min^{-1} of $FeSO_4 \cdot 6H_2O$

Table 2 Mass loss of $FeSO_4 \cdot 6H_2O$ samples during DTA/TG experiments for different heating rates β=1, 2, 5 and 10°C min^{-1}

Step	Heating rate β/°C min^{-1}				$\overline{\Delta m}$ (exp.)/%	Δm (th.)/%
	1	2	5	10		
Dehyd 1	–13.7	–13.9	–13.7	–13.7	–13.8	–13.85
Dehyd 2	–34.7	–33.9	–33.9	–33.8	–34.1	–34.62
Dehyd 3	–41.3	–40.2	–41	–41.3	–41	–41.55
Decomp 1	–52.8	–49.8	–51.2	–52.3	–51.5	–53.8
Decomp 2	–70	–68.9	–68.9	–68.8	–69.2	–69.23

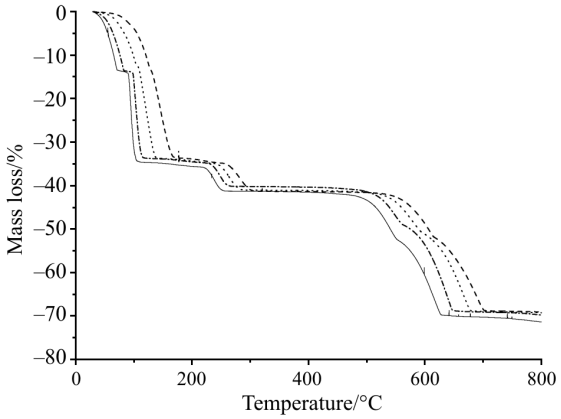

Fig. 3 Mass loss (%) of $FeSO_4 \cdot 6H_2O$ with different heating rates, — – 1, – · – – 2, ··· – 5, --- – 10°C min^{-1}

when the heating rate increases. The processes become less and less sharply separated on the temperature scale. Nevertheless, up to 10°C min^{-1}, the TG and DTG measurements were found very accurate.

For each process, precise temperature determinations were obtained from the peak temperature on the DTG or/and the DTA curves (Table 3). The DTA and DTG peak temperatures are close together within 1 or 2°C whatever the process and the heating rates. In the calculations, DTA or DTG peak temperature will be used indifferently.

Dehydration process

Results of the TG/DTA experiments in the 30–300°C temperature range are presented in Fig. 4. Three well separated mass loss plateaus with the corresponding DTA peaks were obtained. This graph shows that the thermal treatment of pyrite at 300°C should remove all the crystallisation water contained in the sulphate compounds.

Table 3 Summary of the temperature peak T_m (°C) values

Step	Heating rate β/°C min^{-1}				
	1	2	5	10	20
Dehyd 1	71	81	102	124	148
Dehyd 2	96	102	125	147	172
Dehyd 3	240	252	269	280	313
Decomp 1	547	554	580	610	650
Decomp 2	620	637	667	692	717

According to the mass variation measurements, the most probable dehydration mechanism could be described by the three following reactions.

- Dehydration 1:

$$FeSO_4 \cdot 6H_2O \xrightarrow{70–100℃} FeSO_4 \cdot 4H_2O + 2H_2O$$

($\overline{\Delta m}$ (exp.)= –13.8%, Δm (th.)= –13.85%)

- Dehydration 2:

$$FeSO_4 \cdot 4H_2O \xrightarrow{95–190℃} FeSO_4 \cdot H_2O + 3H_2O$$

($\overline{\Delta m}$ (exp.)= –34.1%, Δm (th.)= –34.62%)

- Dehydration 3:

$$FeSO_4 \cdot H_2O \xrightarrow{245–310℃} FeSO_4 + H_2O$$

($\overline{\Delta m}$ (exp.)= –41%, Δm (th.)= –41.55%)

Such a sequence is quite similar to that observed for the other hydrates [20]. Considering the first dehydration step, the thermal signal is strongly asymmetric. It becomes maximum when the reaction is fully achieved. The decomposition rate of the $FeSO_4 \cdot 6H_2O$ dehydration reaction is maximum when it is fully transformed into $FeSO_4 \cdot 4H_2O$. From a kinetic point of view, it could be described as a zero order reaction. On the other hand, the DTA peaks of the two other dehydration steps are perfectly symmetric. We noticed

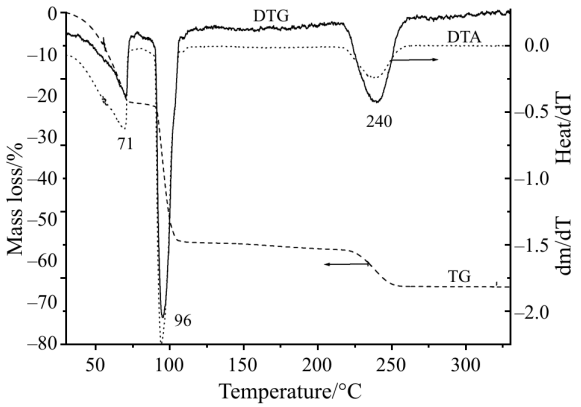

Fig. 4 TG, DTG and DTA curves recorded at 1°C min^{-1} for the dehydration of $FeSO_4 \cdot 6H_2O$

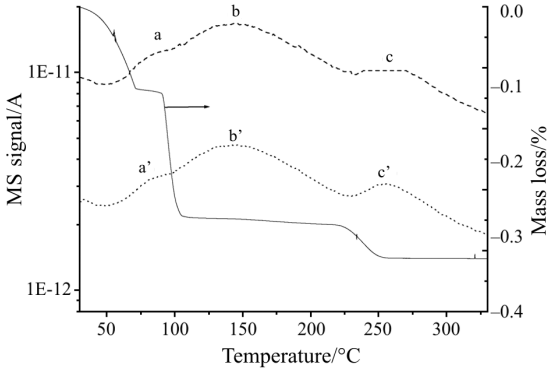

Fig. 5 Coupled mass spectrometry and TG analysis, β=1°C min^{-1}, — – TG, ···,--- – MS signal: *m*/*z*=16 (a,b,c peaks) *m*/*z*=17 (a',b',c' peaks)

that the temperature of DTA peaks maximum matches remarkably the temperature for the half mass variation of the considered step. Usually, this behaviour is typical of a first order reaction. Water evolution was evidenced by mass spectrometry for the three dehydration steps (Fig. 5). The MS signals ascribed to the water released by the samples (mass on charge ratio *z*=16, 17, 18) varied simultaneously in the same amplitude. The intermediate hydrate phases were also identified by XRD analysis and confirmed the mechanism of dehydration of $FeSO_4 \cdot 4H_2O$. These results agree with the previous determination made by Thomas *et al.* [18] by mass spectrometry.

Decomposition process

The thermal decomposition of $FeSO_4$ proceeds via a two-step pathway (Fig. 6). On the ground of the TG measurements and XRD analysis, the mechanism for $FeSO_4$ decomposition to Fe_2O_3 was found to be:

- Decomposition 1:

$$6FeSO_4 \xrightarrow{525–650°C} Fe_2(SO_4)_3+2Fe_2O_3+2SO_2$$

$$(\overline{\Delta m}\ (\text{exp.})= -51.5\%,\ \Delta m\ (\text{th.})= -53.8\%)$$

- Decomposition 2:

$$Fe_2(SO_4)_3 \xrightarrow{625–710°C} Fe_2O_3+3SO_2+3/2O_2$$

$$(\overline{\Delta m}\ (\text{exp.})= -69.2\%,\ \Delta m\ (\text{th.})= -69.23\%)$$

The final product was well identified by XRD as hematite Fe_2O_3 with its typical reddish colour. $Fe_2(SO_4)_3$ was found to be the only intermediate compound during the decomposition of $FeSO_4$. This result agrees with the recent study of Siriwardane *et al.* [17]. This point was correlated by the thermogravimetric analysis data. The experimental mass losses are very close to the values predicted from the proposed decomposition pathway. However, for high heating rates, small differences between our determinations and the expected mass losses were observed. The differences may be ascribed to $Fe_2(SO_4)_3$ decomposition (Decomp 2) occurring before the completion of $FeSO_4$ transformation into $Fe(SO_4)_3$.

By means of mass spectrometry (Fig. 7), sulphur dioxide SO_2 (*m*/*z*=48, 40 and 32) was evidenced as a volatile product issued from the thermal decomposition of the intermediate compound $Fe(SO_4)_3$. These results are similar to those obtained earlier by Thomas *et al.* [18]. Finally, the decomposition reaction of iron sulphate into hematite could be written:

$$FeSO_4 \xrightarrow{525–710°C} 1/2Fe_2O_3+SO_2+1/4O_2$$

For both processes, the DTA and DTG signals were found asymmetric. The maximum of the reaction rates was reached end of the reaction. At high temperature (between 450 and 700°C), the mass spectrometry signals were similar to those recorded with copper sulphate decomposition [21]. The MS signals were typical of transition metal sulphate decomposition. Opposite to dehydration process, the MS signals were well identified even at high heating rates.

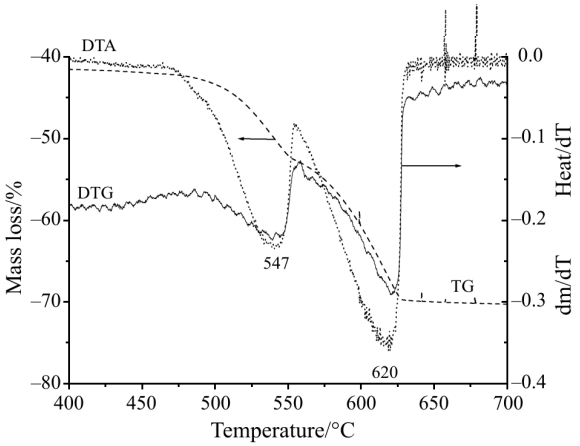

Fig. 6 TG, DTG and DTA curves recorded at 1°C min^{-1} for the decomposition of $FeSO_4 \cdot 6H_2O$

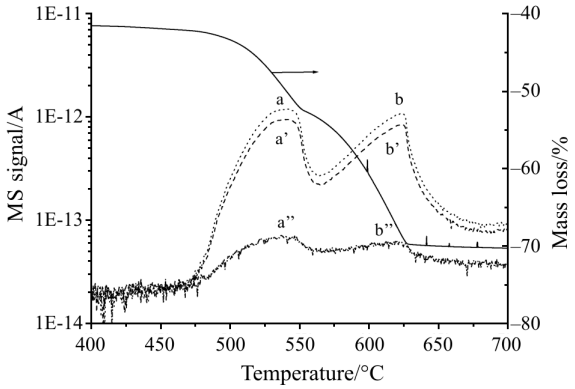

Fig. 7 Coupled mass spectrometry and TG analysis, β=1°C min^{-1}, — – TG, ···,--- – MS signal: *m*/*z*=48 (a,b peaks), *m*/*z*=40 (a',b'' peaks), *m*/*z*=32 (a'',b'' peaks)

In addition, thermal decomposition of $FeSO_4 \cdot 6H_2O$ was studied in a closed oven (but not tightness) under a low flux of inert gas due to the continuous flushing of the glove-box with high purity argon gas. The sample mass was increased (few grams compared to 85 mg) and was placed in quartz container during the heating cycle. In these conditions, $FeOH(SO)_2$ was identified by means of X-ray diffraction. This compound has already been evidenced by Safulin [13] as a decomposition product of $FeSO_4$. It was postulated that the water pressure in the oven could be high enough (residual water from the dehydration steps) to allow a reaction with $Fe(SO_4)_3$. It might be also ascribed to the oxidation of the unreacted $FeSO_4$ with O_2 released during the second decomposition stage [22].

Conclusions

In this work, the thermal stability of hydrated iron sulphate $FeSO_4 \cdot 6H_2O$ (impurity at pyrite surface) was studied by means of coupled thermal analysis and mass spectrometry. Its thermal decomposition proceeds in five steps:

i) three dehydration steps

$$FeSO_4 \cdot 6H_2O \xrightarrow{70-100^\circ C} FeSO_4 \cdot 4H_2O + 2H_2O$$

$$FeSO_4 \cdot 4H_2O \xrightarrow{95-190^\circ C} FeSO_4 \cdot H_2O + 3H_2O$$

$$FeSO_4 \cdot H_2O \xrightarrow{245-310^\circ C} FeSO_4 + H_2O$$

ii) two decomposition steps

$$6FeSO_4 \xrightarrow{525-650^\circ C} Fe_2(SO_4)_3 + 2Fe_2O_3 + 3SO_2$$

$$Fe_2(SO_4)_3 \xrightarrow{625-710^\circ C} Fe_2O_3 + 3SO_2 + 3/2O_2$$

The decomposition of the dehydrated iron sulphate leads to hematite Fe_2O_3. It was pointed out that the intermediate compound formed during the decomposition could be either $Fe_2(SO_4)_3$ (water free atmosphere) or $FeOH(SO)_2$ in presence of residual water.

Acknowledgements

Patrick Masset is indebted to the French Atomic Energy Agency, ASB-Aerospatiale Batteries and LEPMI-INP Grenoble for their financial support. Serge Schoeffert from ASB-Aerospatiale Batteries is deeply thanked for the fruitful discussions we had.

References

1 R. A. Guidotti, Proc. 27th Intern. Sampe Technical Conference, (1995).
2 A. Attewell, Chem. Ind., 5 (1990) 131.
3 S. Dallek and B. F. Larrick, Thermochim. Acta, 95 (1985) 139.
4 J. P. Pemsler, R. K. Lam, J. K. Litchfield, S. Dallek, B. F. Larrick and B. C. Beard, J. Electrochem. Soc., 137 (1990) 1.
5 P. Masset, J. Y. Poinso, S. Schoeffert and J. C. Poignet, Proc. 40th Power Sources Conference, (2002) 246.
6 D. Golodnitsky and E. Peled, Electrochim. Acta, 45 (1999) 335.
7 J. Q. Searcy, P. Neiswander and J. R. Armijo, Tech. Report No. SAND81-1019C (Sandia National Laboratories, 1981).
8 J. Q. Searcy, P. Neiswander, J. R. Armijo and R. W. Bild, Tech. Report No. SAND81-1705 (Sandia National Laboratories, 1981).
9 K. Grjotheim, B. Haugsdal, H. Kvande, H. G. Nebell and T. A. Utigard, J. Electrochem. Soc., 135 (1988) 51.
10 R. C. Wheeler and G. B. Frost, Can. J. Chem., 33 (1955) 546.
11 P. K. Gallagher, D. W. Johnson and F. Schrey, J. Am. Ceram. Soc., 53 (1970) 666.
12 G. Pannetier, J. M. Bregeault and G. Djega-Mariadassou, C. R. Acad. Sci., 258 (1964) 2832.
13 N. S. Safiullin, E. B. Gitis and N. M. Panesenko, Russ. J. Inorg. Chem. (English Trans.), 13 (1968) 1493.
14 M. Huuska, M. Koskenlinna and L. Niiniströ, Thermochim. Acta, 13 (1975) 315.
15 N. Kanari, I. Gaballah, C. Mathieu, N. Neveux and O. Evrard, Proc. EPD Congr., 17 (1999).
16 T. L. Aselage and E. E. Hellstrom, J. Electrochem. Soc. , 134 (1987) 1929.
17 R. V. Siriwardane, J. A. Poston, E. P. Fisher, M. S. Shen and A. L. Miltz, Appl. Surf. Sci., 152 (1999) 219.
18 P. S. Thomas, D. Hirschausen, R. E. White, J. P. Guerbois and A. S. Ray, J. Therm. Anal. Cal., 72 (2003) 769.
19 S. Dallek, Proc. 32th Intern. Power Sources Symp., (1987) 643.
20 A. K. Galwey, Thermochim. Acta, 355 (2000) 181.
21 Balzers Instruments, Mass spectrometer Manual.
22 M. S. R. Swamy, T. P. Prasad and B. R. Sant, J. Thermal Anal., 15 (1979) 307.

Received: July 29, 2005
Accepted: November 7, 2005

DOI: 10.1007/s10973-005-7267-6